CFD Simulation for Predicting Core Inlet Flow Distribution in a 1/5 Scale Model of the APR1000

Uiju Jeong[a*], Yujung Choi[a], Kihwan Kim[b] and Dong-Jin Euh[b]
[a]*SMR Development Lab., KHNP Central Research Institute, 70, Yuseong-daero 1312beon-gil, Daejeon, Korea*
[b]*Atomic Energy Research Institute, 111, Daedeok-daero 989beon-gil, Daejeon, Korea*
[*]*Corresponding author: ujjeong88@khnp.co.kr*

Keywords : APR1000, CFD, core inlet flow distribution, V&V

1. Introduction

Recently, KHNP has been officially selected as the preferred bidder for the Czech Republic's nuclear new build project. The APR1000 reactor, planned to be constructed under the project, is a reactor that combines the proven technologies applied in the APR1400 and OPR1000 with the advanced technologies of the APR+ and EU-APR.

This paper aims to introduce the CFD model developed for the experimental apparatus established as part of the core flow distribution demonstration project, which is being conducted to enhance the safety and licensability of the APR1000. The core flow distributions are defined by the flow at the core inlet and the pressure distributions at the core outlet. The core inlet flow and outlet pressure distributions should be designed to be as uniform as possible across all fuel assemblies, as greater uniformity is beneficial from a thermal and mechanical integrity perspective.

This paper describes the CFD model and its results, focusing on identifying areas for improvement in the current CFD model by comparing and analyzing the CFD results with experimental data. Through this paper, we hope to share the accuracy level of the core flow distribution simulation using a commercial CFD analysis tool.

2. Methods and Results

The CFD model has been developed for a 1/5 scale model of the APR1000 using a commercial CFD software ANSYS CFX. The 1/5 scale model and its calculation results are described. The results are compared and analyzed against the experimental data [1].

2.1 Geometry model

Figure 1 shows a geometry of the 1/5 scale model, mainly consists of six parts such as cold legs, downcomer, lower plenum, core, upper plenum, and hot legs. The lower plenum contains complex structures such as flow skirt and lower support structures, which facilitate flow mixing while also making it difficult to accurately predict the flow. The core consists of 177 core simulators, each of which simulates a single actual fuel assembly, and is specifically designed to have similarity in terms of inlet and outlet pressure drop and crossflow mixing characteristics [1].

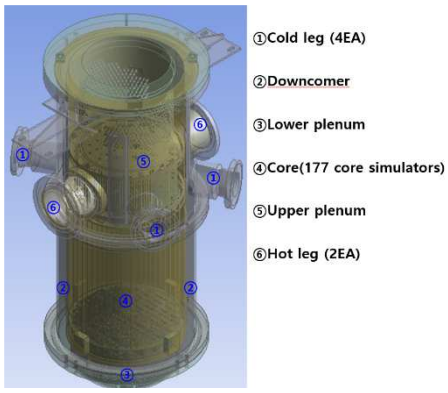

Fig. 1. Geometry of a 1/5 scale model of the APR1000

2.2 Grid model

A grid structure for the geometry model has been made by using ANSYS Workbench mesh program. For convenience, the geometry model was divided into four parts, and grids were generated individually for each part. During the solver setting stage, these grid structures were connected. The initially generated grid model was further improved in quality using the smooth function in the ICEM CFD program. The grid structures are shown in Fig. 2.

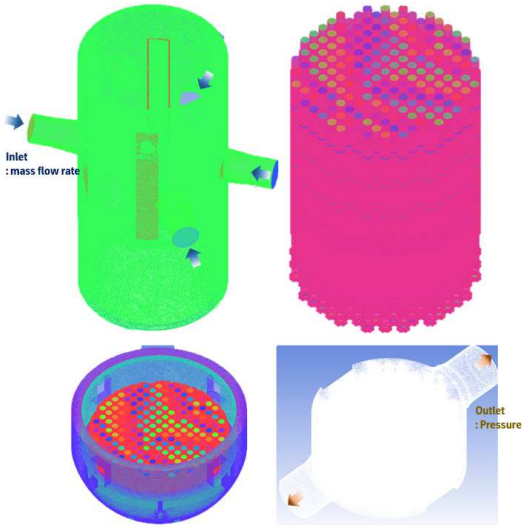

Fig. 2. Grid model of a 1/5 scale model of the APR1000

In a core simulator, four thin perforated plates are installed to simulate differential pressure characteristics. By setting these perforated plates as porous medium domains, the number of mesh cells could be significantly reduced.

Through a grid independence study, an optimized grid model was derived, consisting of approximately 200 million cells.

2.3 Solver settings

Since the flow inside the reactor operates in a fully turbulence regime, the selection of an appropriate turbulence model is crucial. Considering this, a sensitivity analysis of turbulence models was conducted by applying three different turbulence models (standard k-ε, shear stress transport, k-ε EARSM model). Based on this sensitivity analysis, the standard k-ε turbulence model is selected.

The ANSYS CFX software includes a porous media model to simulate flow through domain with porous medium. This model accounts for the impact of the porous medium on the mean flow by incorporating an additional flow resistance term into the momentum equation. While a porous media model can be a powerful tool to simplify the flow domain and reduce the number of mesh cells, it may not accurately simulate detailed physical phenomena. Therefore, in this analysis, its use was limited to the perforated plates in the core simulator.

In this analysis, the porous media employs the isotropic loss model, which requires two parameters, permeability and loss coefficient, to be input. These input parameters were varied iteratively until the CFD calculations yielded results similar to the experimental results of pressure drop along the core simulator and crossflow mixing charateristics between the simulators.

To match the experimental results of crossflow mixing characteristics between the core simulators, the input parameters of the isotropic loss model were set so that a larger pressure drop was generated in the perforated plate closest to the inlet of the core simulator compared to the other plates.

In the steady state simulation, the inlet boundary was set as the mass flow rate with a specific value at 60°C determined by the methdology of scaling analysis, while the outlet pressure was set to 0 Pa. All wall boundaries were defined as non-slip, and the scalable wall function was employed to model the flow behavior near the walls. The calculation was considered to have converged when the RMS residual dropped below 10^{-3}, and both the core inlet flow rates and differential pressure at the core simulators stably converged to specific values.

2.4 Results CFD results and its validation

Most of the results were presented as normalized values. Since the uniformity of the core inlet flow distribution and the pressure drop characteristics at key loop locations are of utmost importance, the standard deviation of the inlet flow rates for all the core simulators and the pressure profiles were presented as the results.

2.4.1 Grid independence study

The grid independence analysis was performed using a fixed turbulence model of SST, and the results are shown in Table I. From these results, it can be seen that the inlet flow uniformity of 'Fine' and 'More Fine' grid models is higher than that of 'Ref.' model. Notably, the flow uniformity observed in the experiment is significantly higher than all of these. Additionally, it was found that the analysis results of grid models 'Fine' and 'More Fine' were more similar to the experimental inlet flow values than those of 'Ref.' model. Consequently, 'Fine' grid model was determined to be the optimal model.

Table I: Standard deviations of different grid models

Grid model	Ref.	Fine	More Fine
Grid Cells	185 M	198M	228M
Std. Devia.	8.36%	8.07%	8.08%

2.4.2 Turbulence sensitivity study

For the turbulence model sensitivity evaluation, the differences between the calculation and experimental values of the inlet flow rate of the core simulator were statistically analyzed. The standard deviations of the flow rate deviations are presented in Table II. Based on these results, the standard k-ε model, which provided results most similar to the experimental data, was selected as the optimal turbulence model.

According to Figure 3, it was confirmed that there is no significant difference in the pressure changes from the cold leg to the hot leg among the different turbulence models.

Table II: Standard deviations of different turbulence models

Case	Exp. - SST	Exp. - Std. k-ε	Exp. - k-ε EARSM
Std. Devia.	5.69%	4.89%	5.51%

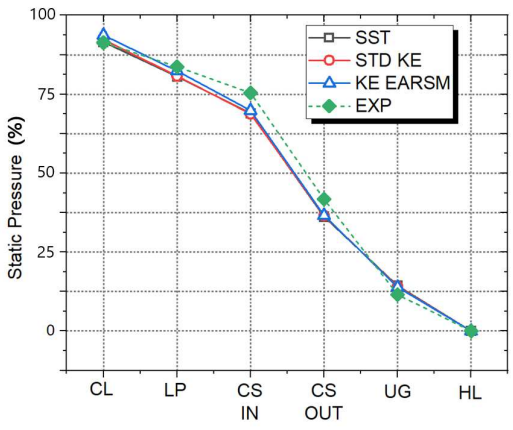

Fig. 3. Static pressure profiles from cold leg to hot leg of different turbulence model

As observed in Fig. 3, the CFD results show a higher pressure drop compared to the experimental data as the fluid enters the core simulator from the lower plenum. Although the cause for this has not yet been clearly identified, it is important to forcus on the phenomenon of 'flow mixing' to explain this. What we can clearly observed from Fig. 4 is that the flow distribution at the core inlet is much more uniform in the experiment compared to the CFD analysis. In other words, less flow mixing occurs in the CFD analysis than in the experiment, leading to a more severe velocity gradient in the CFD analysis. Considering that a larger velocity gradient tends to result in a greater pressure drop, the higher pressure drop observed in the CFD analysis can be explained by the reduced flow mixing, compared to the experiment.

2.4.3 CFD results and its validation

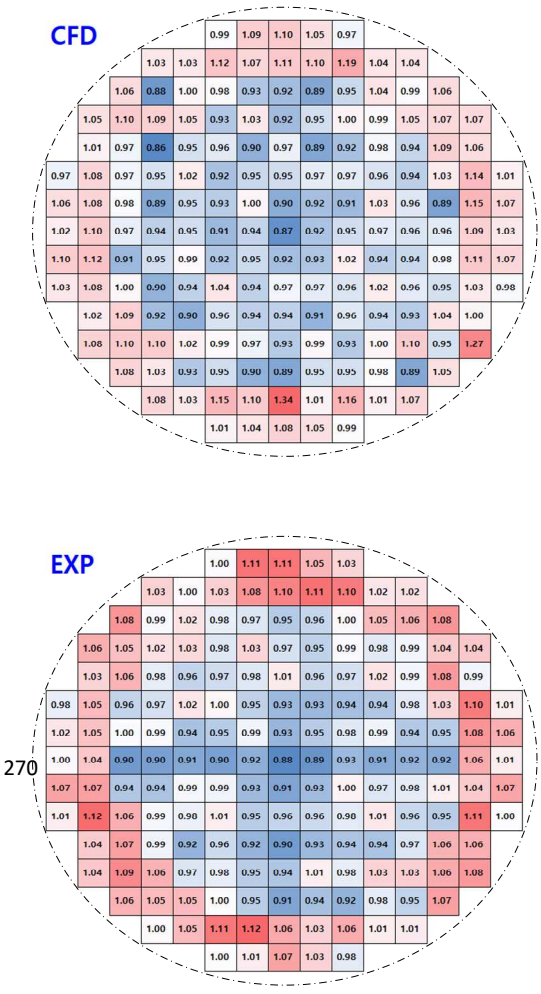

Fig. 4. Core inlet flow distribution from CFD and experiment

Both the CFD simulation and experiments showed similar results, with higher flow rates forming in the outer region and relatively lower flow rates forming in the central region. Howerver, in the flow distribution results from the CFD, it was observed that some specific core simulator exhibited more than a 15% flow deviation compared to adjacent core simulator, which is somewhat difficult to consider as a realistic deviation.

The numerous complex and even asymmetrically arranged structures in the lower plenum make it difficult to accurately predict turbulent flow through a CFD simulation. It is presumed that the significant flow rate deviations among the adjacent core simulators were caused by the limited simulation performance of turbulent behavior, which in turn restricted the flow mixing phenomena. The first basis for this assumption is the fact that the pressure drop occurring as the flow enters the core from the lower plenum shows the greatest discrepancy between the experiment and the analysis, as observed in Fig. 3. The second basis is that the locations where significant flow rate deviations between core simulators occur are mostly in the outer regions of the core. It can be suggested that the flow path from the downcomer to the core outer region is the shortest, which could result in the least flow mixing. The difference in flow path lengths can be observed in the schematic presented in Fig. 5. In the experiment, rapid flow homogenization occurs as the flow passes through the flow skirt and lower support plate. However, in the CFD simulation, it is observed that when the flow path is shorter, sufficient flow mixing does not occur, resulting in less flow homogenization compared to the experiment.

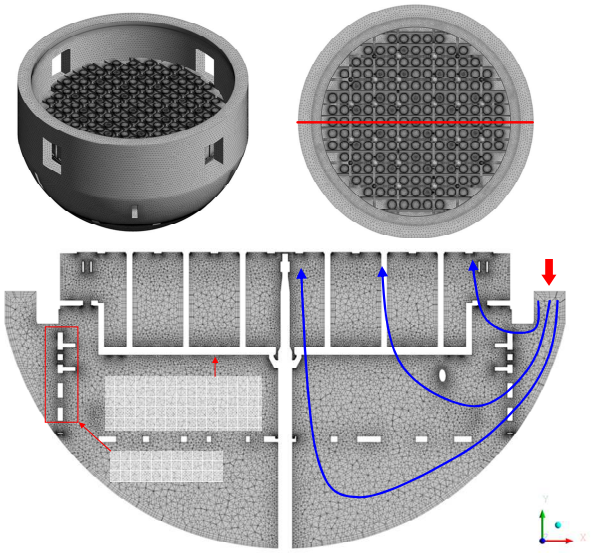

Fig. 5. Lower plenum showing flow path from the downcomer to core inlet

The results of the statistical comparison between the CFD analysis and experimental data regarding the core inlet flow distribution are presented in Table III. Although it was found that the CFD simulation accuracy for the flow distribution in the core outer region is low, as show in Table III, the overall flow differences between the experiment and CFD were within 10% with a 95% confidence interval.

Table III: The statistical results of CFD analysis and experiment regarding the core inlet flow distribution

Case	CFD	Exp.	Exp. - *CFD*
Standard deviations	7.65%	5.59%	4.89%
95% confidence interval	0.85~1.15	0.89~1.11	-9.58% ~ 9.58%

3. Conclusions

In this study, the core inlet flow distribution in a 1/5 scale model of the APR1000 was calculated using the ANSYS CFD code, and it was confirmed that the error compared to the experimental values was within 10%. It is important to note that the accuracy of the CFD results for the inlet flow distribution in the core outer region was somewhat low. This results is presumed to be due to the limitations of the RANS-based turbulence model applied in this CFD anslysis in simulating large eddies. This is because large eddies, which occur when the fluid passes through obstacles or small holes, facilitate rapid flow mixing.

Improving the simulation performance of flow mixing phenomena in the domain between the downcomer and the core outer region is considered a key point for enhancing the predictive accuracy of the core inlet flow distribution.

REFERENCES

[1] K. Kim, W.-S. Kim, H.-S. Choi, H. Seol, B.-J. Lim and D.-J. Euh, An Experimental Evaluation of the APR1000 Core Flow Distribution Using a 1/5 Scale Model, Energies, Vol.17, p. 2714, 2024.

Acknowledgements

The authors would like to gratefully acknowledge the financial support of the Korean Government (MOTIE, Ministry of Trade, Industry and Energy) (No. 20217810100010)